CYBERNETICS AND PHYSICS, VOL. 3, NO. 2, 2014 , 49–54

SIMULATIONS OF ANGIOGRAPHY X-RAY SOURCE BASED ON ELECTRON CHANNELING IN CRYSTALS

T.V. Bondarenko
Department of Electrophysical Facilities
National Research Nuclear University
(Moscow Engineering Physics Institute)
Russia
TVBondarenko@mephi.ru

S.M. Polozov
Department of Electrophysical Facilities
National Research Nuclear University
(Moscow Engineering Physics Institute)
Russia
SMPolozov@mephi.ru

Yu.A. Bashmakov
Laboratory for Accelerator Devices
The Lebedev Physical Institute
of the Russian Academy of Sciences,
Department of Electrophysical Facilities
National Research Nuclear University
(Moscow Engineering Physics Institute)
Russia
Bashm@x4u.lebedev.ru

Abstract

The article concerns the new method of acquiring the narrow-band X-ray energetic spectrum based on the idea of electron channeling in crystals. Polycapillary X-ray filter exploited in this method helps to eliminate the high-energy part of the spectrum and obtain dramatically reduction of the absorbed doses. This method may find a particularly important applications in angiography that has nowadays become the state of the art medical imaging technique for visualization of the blood vessels and organs of the body, with particular interest in the arteries, veins and the heart chambers. X-ray sources in angiography applications are based only on the X-ray tubes that are really well investigated. The main drawback of the tubes is wide spectrum width of the generated radiation. Monochromatic radiation source application can result in better imaging, and, moreover, lower irradiation dose can be applied to a patient.

Key words

Channeling, linac, angiography, crystal, polycapillary.

1 Introduction

Many important and state-of-the-art medical imaging technologies require a high brightness and quasi-monochromatic X-ray source. They are well known as phase contrast imaging (PCI), coherent X-ray diffraction imaging, digital subtractive angiography, dichromography, time-of-flight imaging, mammography in part [Fouras, Kitchen, and Dubsky, 2009; Chen et al., 2011] etc. Monochromatic radiation source results in better imaging, and, moreover, lower irradiation dose can be applied to a patient. As an example, the dose absorbed by patient at the angiography procedure is 180-240 times larger than that at the chest radiography. The main problem is the source broad spectrum.

As known, quasi-monochromatic X-rays cannot be produced using conventional high-voltage X-ray tubes. Four different methods are applicable to produce monochromatic X-rays: synchrotron or undulator radiation [Suortti and Thomlinson, 2003], Compton scattering [Achterhold et al., 2013], K-capture [Harding, 2006] and radiations in aligned crystals (such as channeling radiation, coherent bremsstrahlung, parametric X-ray radiation, etc.) [Freudenberger et al., 1996]. The filtration of the X-ray can also be applied to broad spectrum of the X-ray. For example mosaic crystals can be used to produce quasi-monochromatic X-rays for mammography [Gambaccini et al., 1995] but the quantum efficiency of this technology is tragically low. Large scale accelerators like synchrotrons, storage rings, energy recovery accelerators or linacs can be used for generation of synchrotron and undulator radiations. Compton scattering needs comparatively smaller accelerator but demand high power laser and high accuracy control system in turn. Very high CW

currents up to tens of A are required to excite the K-capturing of La or Ba emitter having considerable photon flux. The emitter life time should be accurately studied also. Channeling radiation CR (and/or coherent bremsstrahlung, CB) source, one of the most powerful radiation types emitted by relativistic electrons in crystals, is discussed below as possible alternative to these techniques.

The idea is to design of a high monochromatic source of X-ray radiation for the energy range near 30-40 keV based on 20-30 MeV electron channeling in crystals for medical applications (especially, for angiography). Two main principles form the base of the discussed source. The first one is realization of the radiation source that would utilize the phenomenon of channeling radiation by relativistic electrons in oriented crystals. The phenomenon is well studied theoretically as well as many dedicated experiments have been performed by various research groups in the world. Another key solution of the source relates to the selection of narrow by energy portion of radiation, mainly free from the hard X-ray radiation tail (one of the main characteristics of incoherent bremsstrahlung). This task is proposed to be done by means of polycapillary optical elements [Kumakhov, 1976]. In reality it means that policapillary optics could be used to deflect selectively defined portion of radiation emitted by the beam of electrons in a crystal (within the energy interval near 33 keV) through rather large angles (10-15 degrees) that would allow the radiation to be delivered to the patient. Both hard tail and soft peak of radiation spectrum remains undeflected in such a way, and, hence, the irradiation dose for the patients becomes much lower.

2 The X-ray Source Scheme

The monochromatic X-ray source based on the channeling radiation generated by the electrons motion inside the oriented crystals is discussed [Bashmakov and Bessonov, 1982]. The principal scheme of the source is presented in the Figure 1. The electron beam (2) is generated in the electron source (1) and accelerated to ultra-relativistic energies in the linac (3) that is not considered in the work. After that electrons pass through the aligned crystal (4) placed inside the goniometer (12) and generated the monochromatic channeling X-ray radiation and broadband bremsstrahlung. The deflecting magnet (5) is used to lead the electron beam to the beam dump (11). The X-ray pass through the polycapillary optics (10) and the radiation with energy lower than 40 keV (9) is filtered and deflected to the patient (7), the rest of the radiation is propagated straightforward to the X-ray dump (6). The radiation is then detected with the X-ray detector (8). The electron beam deflection is done in order to eliminate the possibility of the polycalillary optics damage. The scheme of using the polycapillary optics allows fixing the main problem of such a facility broadband bremsstrahlung spectrum that leads to unnecessary dose enhancement that is obtained by the patient. The accelerator in this scheme is considered to be the conventional medical linac providing following parameter values: current from 1 to 100 mA, beam pulse length μs, energy spectrum near 1 % (can be acquired by additional beamline elements) for 20-30 MeV electrons energy level.

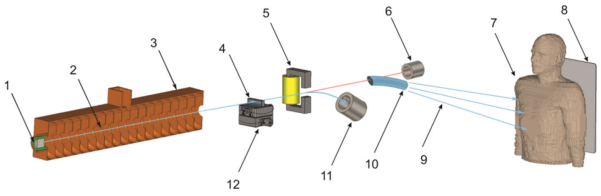

Figure 1. Principal scheme of the proposed X-ray source

3 Simulation of Electron's Motion in Crystals and Channeling Radiation Generation

The channeling is the process of the electron motion inside the crystal between the crystallographic planes (in case of the planar channeling) or near the crystallographic axis (in case of the axial channeling) [Dabagov and Zhevago, 2008]. In the first case electron captured in the channel is moving along the crystal axis and experience the influence of the axially-symmetrical averaged coulomb field of the crystal axis. In the planar channeling the particle is forced by the fields of the atoms situated on the crystalline plane [Bashmakov and Polozov, 2014]. We investigated the planar channeling in the crystal along the $< 110 >$ plane of the diamond due to high efficiency of the X-ray radiation in this case [Lindhard, 1965].

The mechanism of channeling radiation can be described in two principal ways: classical physics model and quantum mechanics. We discussed the planar channeling using the classical physics mechanics. Electrical field formed between the crystallographic planes can be characterized with an averaged potential $U(x)$ where x is transversal offset from the channel central plane. Potential $U(x)$ is smooth, even and periodical function with period of $2d$ (the channel width), known as a reversed parabola [Dabagov and Zhevago, 2008]. The schematic view of such potential and it's polynomial approximation of the potential using the 10^{th} power polynomial are shown in Figure 2 for diamond crystal. Within the classical approximation the electron with energy and rest mass of m is performing small transversal harmonic oscillations relative to channel central plane. If the magnitude of oscillations is much less then channel width ($x_m << d$) the frequency of the oscillations can be expressed as:

$$\Omega_n = \sqrt{2}\Omega_0, \Omega_0 = \frac{c}{d}\sqrt{\frac{2eU_0}{\epsilon}}$$

here $\gamma = \epsilon/mc^2 = (1-\beta^2)^{-1/2}$ is the Lorentz factor, $\beta = v/c$, v - particle velocity. It is obvious that the

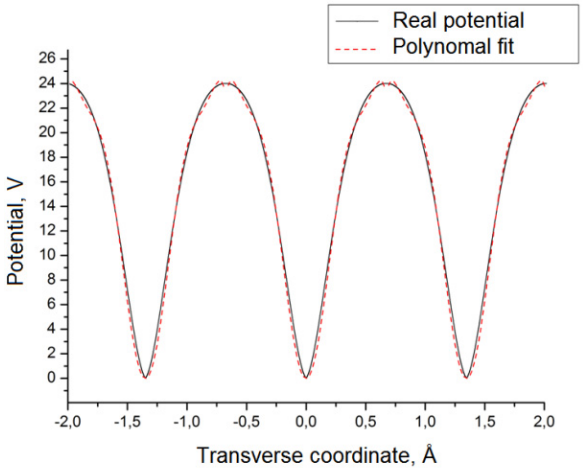

Figure 2. Schematic view of diamond crystal potential [Lindhard, 1965].

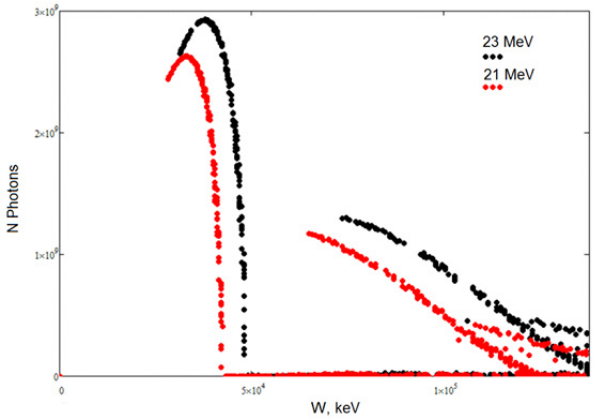

Figure 3. Spectrum of the channeling radiation.

frequency of transversal oscillations is reduced with energy gain as $\sim \gamma^{-1/2}$ [Lindhard, 1965]. If the particle oscillation has large magnitude compared to channel, the frequency of the oscillations is becoming dependent on the magnitude [Alferov, Bashmakov and Cherenkov, 1989]. The numerical simulation of electrons dynamics and channeling radiation generation was done by means of BEAMDULAC-CR code [Bashmakov and Polozov, 2014]. The code was tested for different types of the targets and various energies of electrons in 10-60 MeV energy band. The results of the experimentally measured peaks positions and their widths together with data obtained from the theoretic estimations and BEAMDULAC-CR code are shown on the Table 1. Theoretical estimations were held using the well-known dependences of the X-ray energy from the Lorenz factor [Genz et al., 1996] for the experimental data acquired from [Kein, Kephert et al., 1985; Gouanere, et al., 1982]. The results reveal that peak position results differ from experimental results less than 10 % in the whole energy band that is a pretty fine accuracy for classical approach.

Table 1 Comparison of the experimental, analytical and BEAMDULAC-CR code radiation parameters.

Electrons energy, MeV	Experiment, keV	Theory, keV	Code, keV
21	33.0±2.4	33.0±2.4	33.1±7.2
16.9	23.0±1.7	24.1±1.6	24.2±5.5
30.5	60.1±3.0	57.1±5.0	59.6±10.0
54.5	161.0±10.3	135.0±15.7	141.0±30.6

Acquired spectrums of the channeling radiation from BEAMDULAC-CR are shown in the Figure 3. The photons number is based on the 10^12 electrons in the single bunch and the diamond crystal thickness of 55 μm. The graphs were evaluated for the 21 and 23 MeV electron energy and correspond to the energy spectrum of the main harmonics 33 ± 2.4 keV (21 MeV) and 37 ± 2.9 keV (23 MeV). The electrons dynamics in the crystal also shows that electron beam should have the divergence around 10 mrad and energy spectrum $\Delta E/E \sim 1\%$ in order to eliminate the dechanneling (travelling of the electrons from one channel to another) of the electrons. For a better understanding the graphs of the electron beam filling three full potential channels travelling with 3 mrad (left) and with 30 mrad (right) for 23 MeV beam energy are presented (Figure 4). The graphs of transverse coordinates and transverse velocities are showing that the 30 mrad case leads to a large number of particles that start to travel from one channel to another right after crystal surface (zero longitudinal position). The phase trajectories plots are showing that a lot of trajectories are not looped that corresponds to dechanneled particles. The percentage of the dechanneled particles vs. divergence is shown in the Figure 5.

4 Bremsstrahlung Simulation

Unfortunately electrons travelling in crystal produce not only coherent channeling radiation but incoherent bremsstrahlung also. The bremsstrahlung X-ray radiation generation process was investigated applying the Monte Carlo based code PyPENELOPE [Acosta, Llovet and Salvat, 2002]. The analyzed target is presented by the 55 μm thick diamond target with 3.5 g/cm^3 carbon density irradiated by the 21 and 23 MeV electron beam correspondingly. The acquired data is presented in the form of photon emission probability (Figure 6). The data shows that emitted bremsstrahlung X-ray radiation has broad energy spectrum with maximum intensity at the energy around 4.5 keV. The bremsstrahlung band starts from energy lower than 1 keV and spreads up to the electron beam energy. Here also the iodine and water attenuation coefficients are shown. It is easy to see that the beast image contrast will be for the X-ray with K-line energy of the iodine.

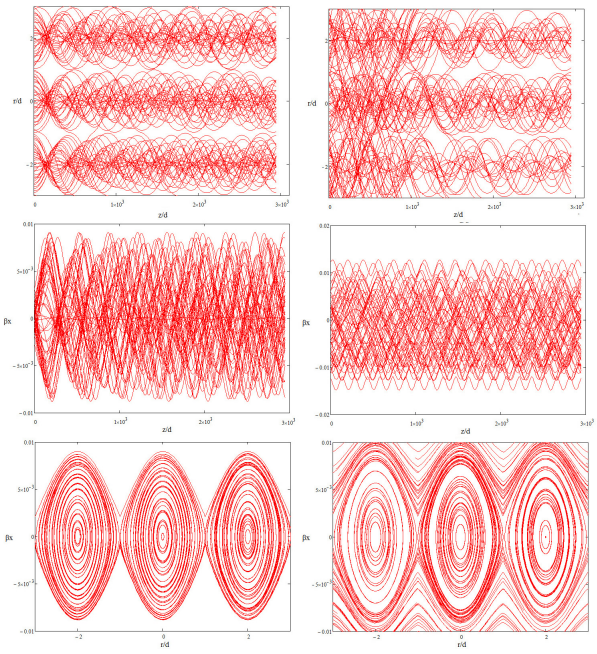

Figure 4. Graphs describing the beam trajectories inside the diamond crystal for 3 (left) and 30 mrad (right) beam divergence: particles trajectories (top), transverse particle velocities (center) and phase trajectories at $(x/d, z/d)$ phase plane (bottom)

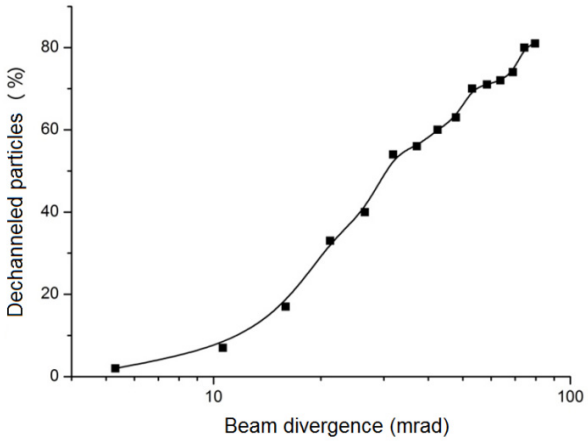

Figure 5. Dechanneled electrons amount vs. beam divergence.

5 Beam Dump and Polycapillary Optics

Beam dump is positioned with a certain deviation from initial electron trajectory and can be performed in the form of the Faraday cup. To deflect electrons from their trajectory the magnetic field should be applied. The deflection in the discussed case is based on the simple but effective magnetic system. It should deflect the beam for and $\psi = 45^\circ$ angle vs. the initial trajectory. Here the magnet with 5x5 cm poles is discussed with application to the 23 MeV beam. To deflect this beam to 45° the 24 mT induction is required.

Induction of this field is not a problem, but arising

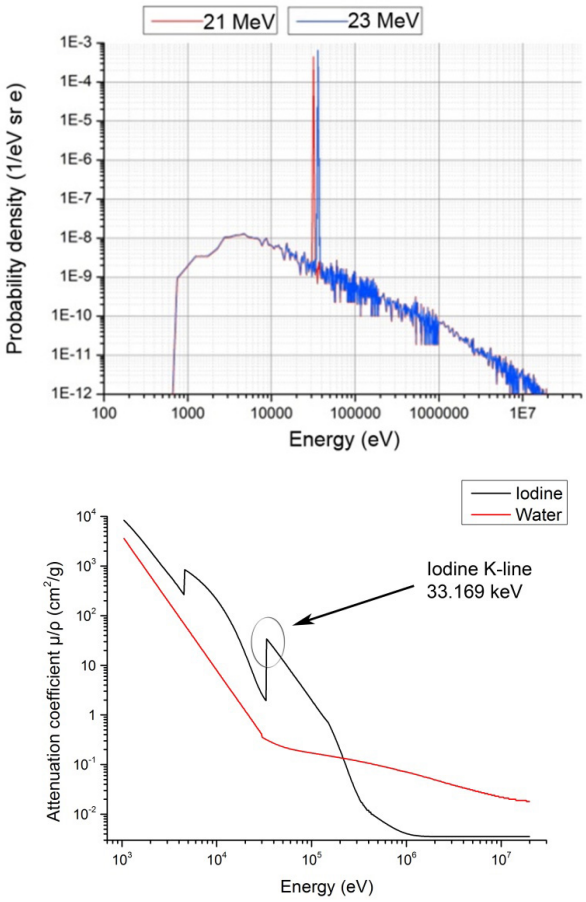

Figure 6. X-ray spectrum for CR source including bremmstrahlung component (top) and attenuation spectrum for iodine and water (bottom)

synchrotron radiation is the one to be investigated. For better interpretation the directivity of the synchrotron radiation is presented in the Figure 7a. The arising radiation has directivity of $\psi + \varphi$, but only the φ part should be taken into account because all other angles are not coming to the input of the optics. The dependence of the radiation vs. the magnetic field induction is presented on the Figure 7b. So while deflecting the 23 MeV beam the arising radiation has power of 10.72 W and energy of 0.2 keV due to equations for the synchrotron radiation. The parameters of the radiation allow concluding that it can be excluded from the discussion due to low energy that makes it fully absorbable by the air. The necessary X-ray band separation is proposed to process using the polycapillary optical system. In principal the X-ray optics based on the single capillary works similar to the fiber optics guiding the radiation of the certain energy through itself. The typical X-ray optics is now manufactured with the μm sizes of the capillaries with length of $\sim$cm and can guide 40 keV X-ray through itself with 40 % efficiency [Kumakhov and Komarov, 1990]. The worst drawback of such optics is the small capture angle of such system that lies

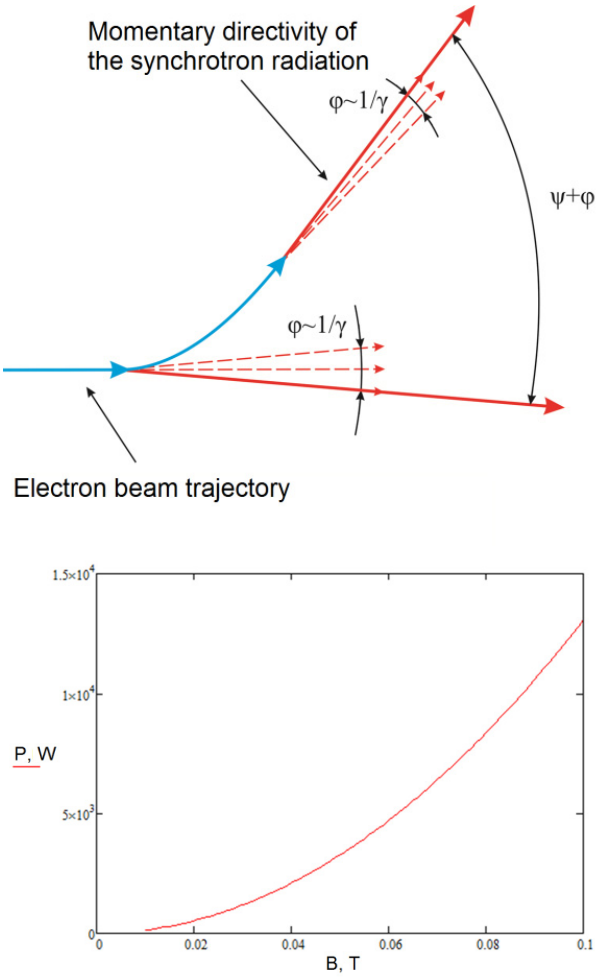

Figure 7. Synchrotron radiation directivity (top) and power vs. magnetic field induction (bottom)

within 0.1 rad that makes them very ineffective for application to X-ray but quite effective for CR-radiation source due to small cone directivity. The X-ray lenses geometry and general design can be found in the article [Kumakhov and Komarov, 1990].

6 Estimated Dose Simulation

For estimation of the absorbed doses and image contrast the X-ray radiation attenuation in the tissue-equivalent phantom was investigated via the Beer-Lambert law. The phantom represents the water cube with the 30 cm edge and a cylindrical cavity with 1 mm diameter containing the 10 % iodine contrast agent (Figure 8). The photons number was calculated via the probability density curves shown on the Figure 1 using 10^{12} electrons. The data for photons yield shows the amount of the photons that fell on the phantom surface after passing the X-ray optics for CR radiation sources and without using any for X-ray tube. Polycapillary optics employment in case of 21 MeV channeling radiation source allows reducing dose acquired by the phantom 54 times vs. the generation system without optics and gives 43 μSv with $2.28 \cdot 10^{11}$ photons. Analogous system with 23 MeV electron source gives 30 times dose reduction and gives 81 μSv with $3.78 \cdot 10^{11}$ photons. The conventional 100 keV X-ray tube with W-Re anode provides 5.6 μSv at $2.2 \cdot 10^{10}$ photons. All data are presented in the Table 2.

Table 2. Photons yield, dose and contrast for different sources types.

Source	Photons number	Absorbed dose, μSv	Contrast (relative)
CR (21 MeV)	$2.2 \cdot 10^{11}$	43	0.8
CR (23 MeV)	$3.8 \cdot 10^{11}$	81	3.0
Tube (100 keV)	$2.2 \cdot 10^{10}$	5.6	1

Contrast of the X-ray tube image is set as 1 to normalize the CR radiation source results. The contrast of iodine-filled cavity measured in these three cases shows that the 23 MeV channeling radiation source gives 3 times higher contrast image of the cavity than the conventional X-ray tube. The 21 MeV channeling source provides lower contrast of the iodine-filled cavity (0.8 of the X-ray tube image contrast) because the maximum channeling intensity peak of the radiation lies in the area of small iodine attenuation coefficients. In both cases the dose normalized by the photon flux value stays practically the same as for X-ray tube.

7 Conclusions

The X-ray source that is based on the channeling radiation principle utilizes the electron beam of 20-30 MeV energy and implies the diamond crystal plate target. Such X-ray source is particularly interesting in application for angiographic procedures that demand narrow-band X-ray radiation.

The investigation of the electron dynamics in the diamond was held with classical approach representing the electron oscillations in the transverse potential field of crystal lattice. The BEAMDULAC-CR code used for calculations also analyzes the X-ray spectrum of the radiated X-ray. The results acquired by the code have fine correlation with experimental works and shows the applicability of such an approach and this code.

The presented X-ray source can provide three times higher contrast of the image than conventional 100 keV X-ray tube using the 23 MeV beam and 55 μm diamond plate. The absorbed dose normalized by the photon flux stays the same as for the X-ray tube. The polycapillary optics used the source effectively filters all the high energy X-ray radiation and transmits channeling X-ray with 40 % efficiency.

The absorbed dose analysis revealed that 23 MeV electron source provides dose of 81 μSv with $3.78 \cdot 10^{11}$ photons that in turn is acquired by using the electron beam with 10^{12} photons in it. The contrast of the iodine filled cavity in the tissue-equivalent phantom for this case three times exceeds the contrast in case of using the 100 kV X-ray tube with the same dose rate.

References

Fouras, A., Kitchen, M.J, and Dubsky, S. (2009) *J. Appl. Phys.* **105**, 102009.

Chen, B., Zhang, F., Berenguer, F. et al. (2011) *New Journal of Physics* **13**, 103022.

Suortti, B., and Thomlinson, W. (2003) *Phys. Med. Biol.* **48**, R1.

Achterhold, K., Bech, M., Schleede, S. et al. (2003) *Nature Scientific Reports* **3**.

Harding, G. (2006) Monochromatic x-ray source *Patent* EP1102302 B1.

Freudenberger, J., Genz, H., Groening, L. et al. (1996) *NIM A* **119**(1–2), pp. 123–130.

Gambaccini, M., Taibia, A., Del Guerra, A. et al. (1996) *NIM A* **365**(1), pp. 248–254.

Kumakhov, M.A. (1976) *Phys. Lett A*, **57**, 17.

Bashmakov, Yu.A., and Bessonov, E.G. (1982) *Rad. Eff.* **66**, pp. 85–94.

Dabagov, S.B., and Zhevago, N.K. (2008) *RIVISTA DEL NUOVO CIMENTO* **31**(9), pp. 491–529.

Bashmakov, Yu.A., and Polozov, S.M. (2014) *Problems of Atomic Science and Technology. Series "Nuclear Physics Investigations"*, **3**(91), pp. 134–137.

Lindhard, J. (1965) *Kgl. Dan. Vid. Selsk. Mat.-Fys. Medd.* **34**(14).

Alferov, D.F., Bashmakov, Yu.A., and Cherenkov, P.A. (1989) *Sov.Phys.Usp.* **32**, p. 200.

Genz, H., et al. (1996) *Physical review B* **53**(14), pp. 8922–8936.

Kein, K.R., Kephert, J.O., Pantell, R.H., et al. (1985) *Physical review B* **31**(1), pp. 68–92.

Gouanere, M., et al. (1982) *Nucl. Instrum. Methods* **194**, p. 225.

Acosta, E., Llovet, X., and Salvat, F. (2002) *Appl. Phys. Lett.* **80**, pp. 3228–3330.

Kumakhov, M.A., and Komarov, F.F. (1990) *Phys. Rep.* **191**, pp. 289–350.